Simulation of a Discharge for the NCSX Stellarator

E.A. Lazarus,
Oak Ridge National Laboratory, Oak Ridge, Tennessee, USA
M.C. Zarnstorff, S.R. Hudson, L-P. Ku, D.C. McCune,
D. Mikkelsen, D.A. Monticello, N. Pomphrey, and A.H. Reiman
Princeton Plasma Physics Laboratory, Princeton, New Jersey, USA

Abstract: We demonstrate that there exists a plausible evolution of the discharge from the vacuum state to the desired high beta state with the self-consistent bootstrap current profile. The discharge evolution preserves stability and has adequate quasi-axisymmetry along this trajectory. The study takes advantage of the quasi-axisymmetric nature of the device to model the evolution of flux and energy in 2D. The plasma confinement is modeled to be consistent with empirical scaling. The ohmic circuit, the plasma density, and the timing of the neutral beam heating control the poloidal flux evolution. The resulting pressure and current density profiles are then used in a 3D optimization to find the desired sequence of equilibria. In order to obtain this sequence active control of the helical and poloidal fields is required. These results are consistent with the planned power systems for the magnets.

I. Introduction

We demonstrate in this paper that there exists at least one plausible discharge trajectory from the vacuum state to the desired NCSX [1] target equilibrium within the constraints of the engineering design. We take advantage of the quasi-symmetry and model the evolution of the plasma current and pressure in 2D.

The resulting profiles of current density and plasma pressure are repatriated to 3D in that a free boundary equilibrium solution is found using the VMEC [2] code. In general, such a solution will have lost the desirable stability and quasi-symmetry features of the reference equilibrium. A series of optimizations with the STELLOPT code [3] will restore these properties in a manner consistent with the engineering constraints. If these properties cannot be recovered then either the choice of discharge trajectory was poor or the coil design is not adequate to the task. Finally the resultant time series of equilibria is examined for flux surface quality with the PIES [4] equilibrium code.

II. Modeling the temporal evolution in 2D

The first task is to create the "equivalent tokamak". The first step is to obtain a current density equivalent of the vacuum transform for the toroidally averaged plasma shape. The "vacuum" equilibrium flux surfaces and current profile of the equivalent tokamak are shown in Fig. 1. This current profile will be modeled as a fixed current driven by an unspecified external source. That source implicitly varies in such a way as to maintain this current profile and not interact in any way with the remainder of the plasma properties. This represents our vacuum state from which we initiate the temporal evolution shown in Fig. 2.

The modeling of the pressure and current profiles is done using TRANSP. [5] The density profile and Z_{eff} are specified in a way consistent with observations in small stellarators and tokamaks. The plasma current has two distinct components: The 321 kA equivalent of the vacuum iota is simulated as an externally specified, unchanging lower hybrid driven current (LHCD) profile. TRANSP allows this driven current profile input to be completely specified, without any other modeling of the standard LHCD process. The simulations are done iteratively: do a run, look at results, change something and do it again -- very much like running an experiment. In order to obtain a current profile that is single valued and rising with increasing toroidal flux at the end of the 300 ms NBI pulse, it is quite important to minimize the Ohmic current during startup. When the plasma is cold, the current diffuses rapidly to the core. Once the plasma heats it will take a very long time to dissipate the Ohmic flux. The plasma current waveform, $I_P(t)$, represents a number of iterations where the old waveform is replaced with a new one, all intended to balance the OH current profile with

neutral beam current drive (NBCD) so the dominant term is the bootstrap current. The neutral beam injection (fig. 2) is already a balance of co & counter beams, however this does not provide precise local cancellation across the plasma. During this iterative procedure an internal feedback loop

in TRANSP is used to adjust the confinement time, to match a chosen global confinement scaling. Both χ_e and χ_i are adjusted to do this, by adjusting an anomalous diffusivity that is summed with analytic calculations of the neoclassical and helical ripple contributions to transport. The radial profile of the anomalous diffusivity is assumed to be flat, as is observed in many stellarator experiments. The global scaling we have adopted is the minimum of neo-Alcator [6] and ITER97 L-mode scaling. [7]

$$\tau_{97L}^{h} = 0.023 \cdot I_P^{0.96} B_t^{0.03} \kappa^{0.64} R^{1.83} (R/a)^{0.06}$$
$$\bar{n}_e^{-0.04} M_{eff}^{0.02} P_{loss}^{0.073}$$
$$\tau_{neoAlc} = 0.019 \cdot \bar{n}_e R^{2.04} a^{2.04}$$
$$(units: \quad s \quad m \quad MA \quad MW \quad 10^{19} m^{-3} \quad T \quad AMU)$$

Thus confinement is neo-Alcator at the beginning of the discharge and switches to ITER97L when the loss power becomes sufficiently large. Also, a switch is set in TRANSP to prevent the LHCD from experiencing the toroidal electric field, incorrectly developing Ohmic power.

The balance of the neutral beam powers is adjusted so that the larger counter-injection losses are compensated by a lower co-injected power. This is done so the effect of NBCD on central iota is not too severe, while overall the NBCD is not too negative. Co-injection orbit losses are about 18% and counter-injection losses are about 30%. While the NCSX program will include an upgrade of the neutral beams to long pulse, initially they will be limited to a pulse length of 0.3 s. The neutral beam pulses are modulated to control the heating power and adjusted, along with the plasma density, so as to produce the desired β_T. The electron density profile is somewhat flat as is common in small stellarators.

In summary, the inputs are the current or loop voltage programming, the plasma density programming, the time variation of the co an counter neutral beam power and the choice of energy confinement scaling. The outputs are the plasma pressure (including the fast ion component) and the current density profile as functions of time. Examining the quantities in Fig. 3, we can see that the device is similar to an advanced tokamak with q_0=2.5 and q_a=1.5. However, the transform related to I_{EXT} is produced by 3D shaping, rather than RF current drive.

III. Repatriation of 2-D results to the stellarator

Having obtained a self-consistent evolution of pressure and current density, we need to follow this path in a sequence of 3D free-boundary equilibria. The input profile functions for VMEC are the pressure, p(s) and flux-surface averaged current profile, I'(s), where $s=\Phi^2$ is the normalized toroidal flux. p (Φ), and $\langle J\rangle(\Phi) - \langle J_{EXT}\rangle(\Phi)$ are extracted from the TRANSP simulation for multiple time slices and fit to Φ^2 to obtain the desired input functions. The 3-D free-boundary equilibria are generated using VMEC.

We then proceed through a series of optimizations to physics targets such as kink stability, ballooning stability, and effective ripple, a measure of quasi-symmetry by variation of coil currents. We should not expect to reproduce the reference (li383) case [8], rather, we want see that the good physics characteristics of the reference can be maintained over the entire discharge with the proposed coil set.

For the cases discussed in this section, we did a full optimization over aspect ratio, R·B, quasi-symmetry, the N=0 & N=1 families of ideal (no wall) kink instabilities and ballooning stability. No attempt is made to minimize the total ampere-turns of the coil currents. We did force the plasma to fit within the vessel. Results from 30 to 400 ms are presented in Table 1.The simulation uses 25 ms to start, so the physical time is time-25 ms A growth rate for the kink of $< 1\cdot 10^{-4}$ is considered negligible, that is, with minor changes in discharge programming it can be avoided. This is satisfied for all cases. The reference case is ballooning unstable in a few zones near the shearless region (43, 45,46 out of 49 zones). Ballooning is evaluated on field lines beginning both at $N_{fp}\Phi = 0°$ and 60°. All the time slices in the simulated evolution *are* ballooning stable. Results are shown in Table 1. Kink growth rates are all smaller than 1.e-4, which is considered negligible. The ripple diffusion ($\Phi^{3/2}$) is also well below a value where ripple loss

would be a significant contribution to the total heat diffusivity. The results for the fixed boundary li383 reference case are added at the bottom of the table. "Ballooning Φ unstable" in the table is the sum of the growth rates in the unstable radial zones. The time evolution of principal quantities is shown in Fig. 4 and profiles at selected times are shown in Fig, 5. These are the profiles that arise from the simulation. The optimization over coil currents alters the shape of the plasma. Regaining kink stability seems the most important part of this procedure. In Figure 6 we show what has happened. The pressure and current density from the 2D simulation are preserved, so a shape change will appear in iota. It is not surprising that the shape change has increased the shear, thus improving stability. Of course, the change is a 3D change in shape so it also served to restore quasi-symmetry.

IV. Summary

We have produced a discharge trajectory that meets the requirements for NCSX. The discharge is stable to low-n and ballooning modes, has adequate quasi-symmetry, reaches the desired Φ, and fits within the first wall of the vacuum vessel. The required coil currents and their time derivatives are within the specifications for the coils and power systems. We have other discharge programming that was nearly as successful. We have not examined flux surface quality with PIES for this particular sequence, but similar sequences have been found to be satisfactory. [9] Implicit in this work is the assumption that the helical field (modular coil currents) as well as the poloidal field varies in time. As was noted above, constant helical field does not yield a stable trajectory. A consequence is the need for control of the plasma

boundary shape, with the desired shape, itself, dependent on the current profile. A more complete report on this work will be published elsewhere. [10]

Acknowledgments

This research was supported by the US Department of Energy under Contract DE-AC05-00OR22725 with UT-Battelle, LLC.

References

[1] M. C. Zarnstorff, et. al., Plasma Physics and Controlled Fusion **43:12A** (2001) A237.

[2]S.P. Hirshman & J.C. Whitson, Phys. Fluids **26**(1993)3553.

[3] S. P. Hirshman, et al., Phys. of Plasmas, **6**(1999)1858.

[4] A. Reiman and H.S. Greenside, Comput. Phys. Commun. **43**(1986)157.

[5] R.J. Hawryluk, in *Proceedings of the Course in Physics of Plasmas Close to Thermonuclear Conditions*, Varrena, 1979 (Commission of the European Communities, Brussels, 1980). Vol. 1, p. 19.

[6] R. R. Parker, Nucl. Fusion, **25** (1985) 1127

[7] Kaye,S., et al., Nuclear Fusion **37** (1997) 1303.

[8] A. Reiman, et.al., Phys. Plasmas **8**(2001)2083.

[9] S. R. Hudson, et al, Nucl. Fusion, **43** (2003) 1040.

[10] E.A. Lazarus, et al, "Simulations of Possible Discharge Evolutions for the NCSX Stellarator," submitted to Fusion Science and Technology.

TABLE:

Time (ms)	Aspect Ratio	Plasma Current (A)	beta %	Distance to wall (m)	Ballooning Σunstable	N=1 Kink Family (□ <0 stable)	N=0 Kink Family (□ <0 stable)	Effective Ripple □$_h^{3/2}$ (s=0.3)
30	4.431	2.23E+01	0.006	4.58E-03	0	0	0	4.55E-04
50	4.65	4.89E+03	0.156	-2.57E-03	0	0	0	1.19E-04
70	4.444	1.20E+04	0.315	5.04E-03	0	0	0	1.36E-04
80	4.474	1.80E+04	0.471	4.78E-03	0	0	0	1.37E-04
100	4.436	1.82E+04	0.428	4.85E-03	0	0	0	1.15E-04
110	4.576	1.85E+04	0.527	4.30E-03	0	0	0	1.33E-04
119	4.426	1.97E+04	0.612	3.79E-03	0	0	0	2.04E-04
138	4.489	2.38E+04	0.793	2.21E-03	0	0	0	1.33E-04
159	4.427	3.11E+04	1.17	9.01E-03	0	0	0	2.69E-04
190	4.37	5.02E+04	1.76	4.86E-03	0	0	0	1.97E-04
220	4.371	6.51E+04	2.16	5.03E-03	0	0	0	2.71E-04
250	4.378	7.67E+04	2.41	4.98E-03	0	2.72E-06	0	2.64E-04
280	4.458	9.38E+04	3.55	4.71E-03	0	3.73E-05	0	5.42E-04
310	4.581	1.08E+05	4.07	4.92E-03	0	5.93E-06	0	6.80E-04
338	4.504	1.18E+05	4.20	2.64E-03	0	8.23E-05	8.75E-05	3.23E-03
369	4.592	1.25E+05	4.48	4.67E-03	0	2.68E-05	0	1.21E-03
399	4.544	1.30E+05	4.53	5.32E-03	0	2.16E-05	0	5.75E-04
LI383	4.365	1.75E+05	4.25	1.49E-02	1.41E-02	0	0	2.17E-05

Table 1. Optimization Results at R·B=2.05 m-T

FIGURES:

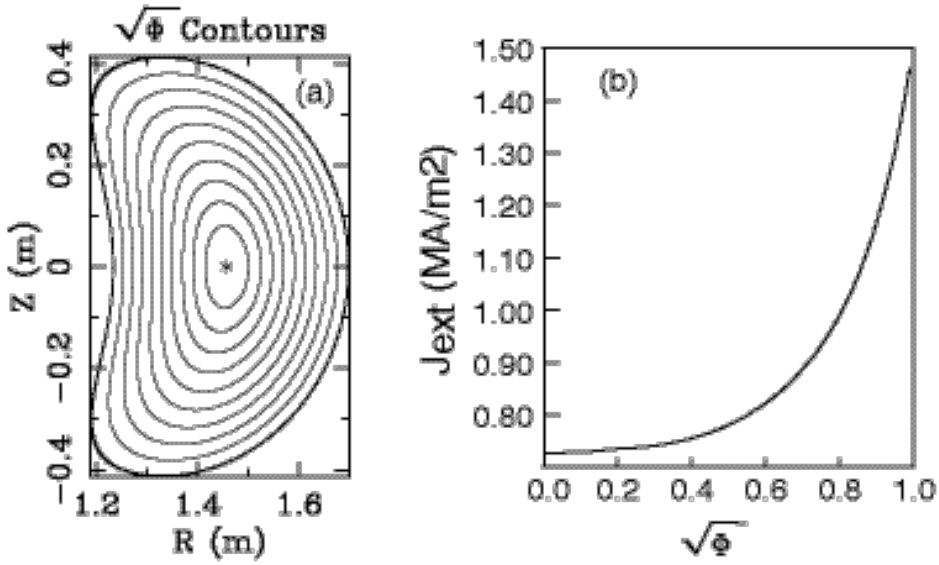

Figure 1. (a). Flux surfaces for the equivalent tokamak and (b). The toroidal current density producing the vacuum transform of the reference configuration in the absence of 3D shaping.

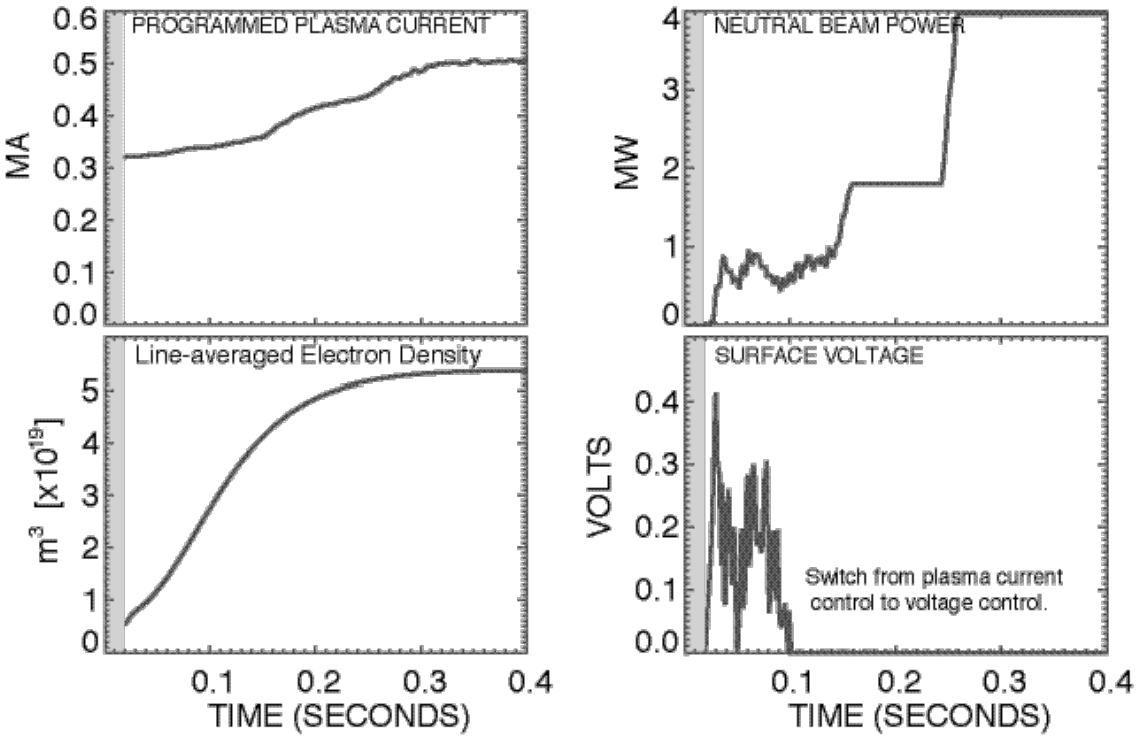

Figure 2. Inputs to 2D modeling: (a). programmed plasma current, (b) neutral beam power, (c) plasma density and (d). the surface voltage, programmed after 0.1 s.

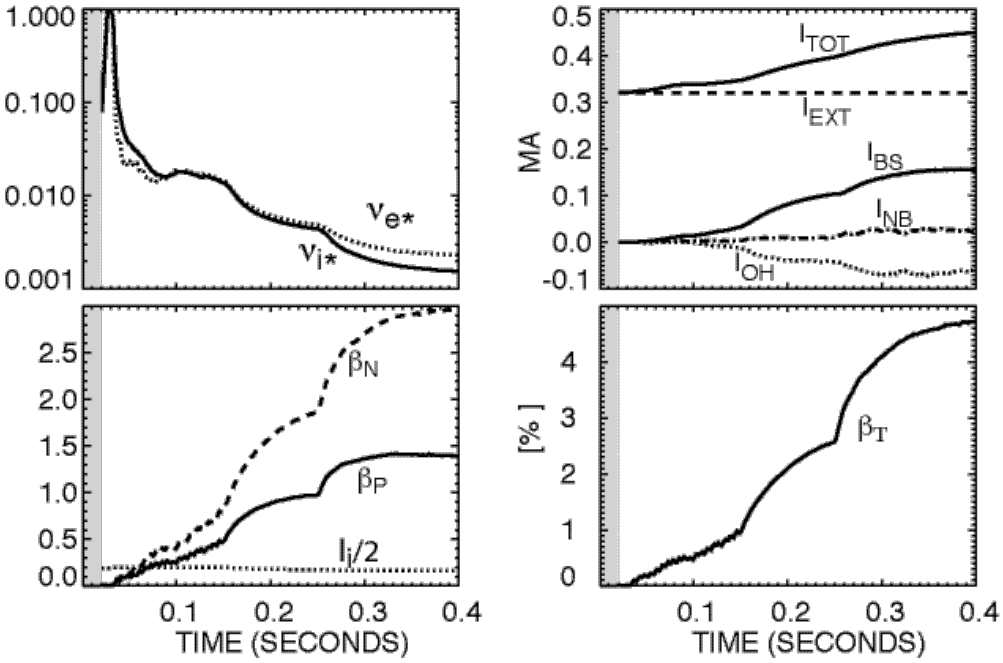

Figure 3. 2D modeling outputs (a). neoclassical collisionalities at half-radius, (b) the components of the plasma current, (c) beta and inductivity and (b). the toroidal .

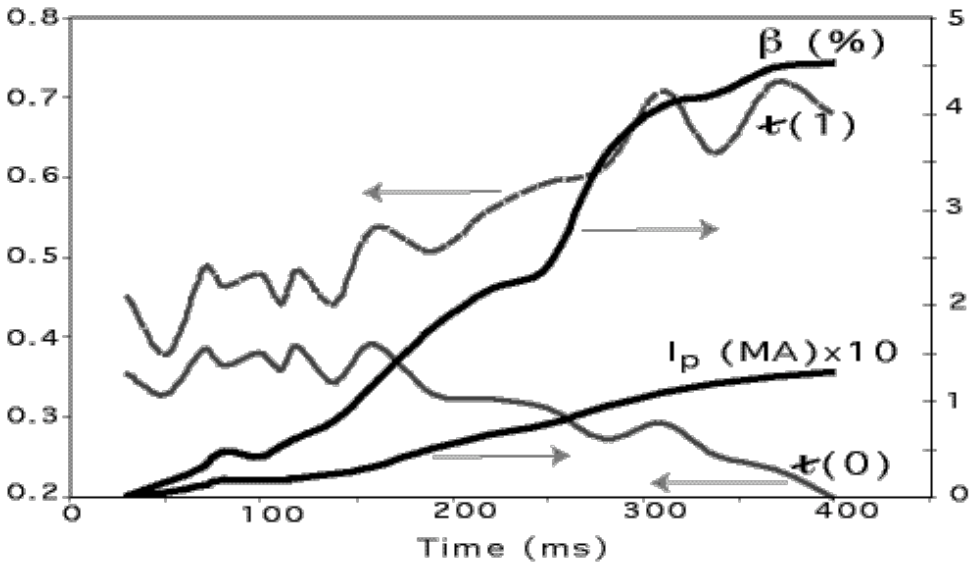

Figure 4. Optimization Results: Evolution of selected quantities at R·B=2.05 m-T. Shown are ι at the axis and boundary (left scale) and I_P, β (right scale).

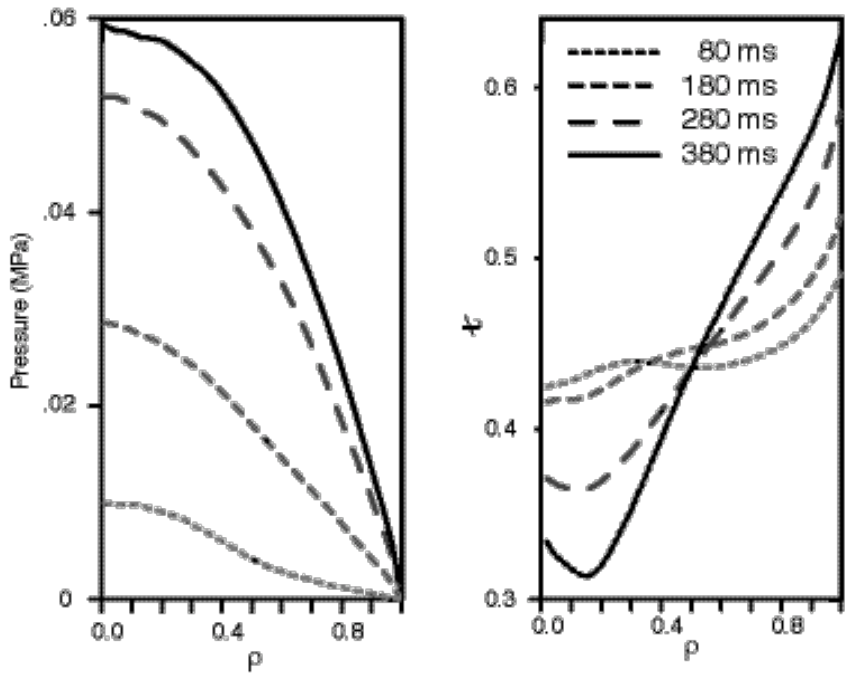

Figure 5. Plasma pressure and transform profiles at selected times from 2D simulation.

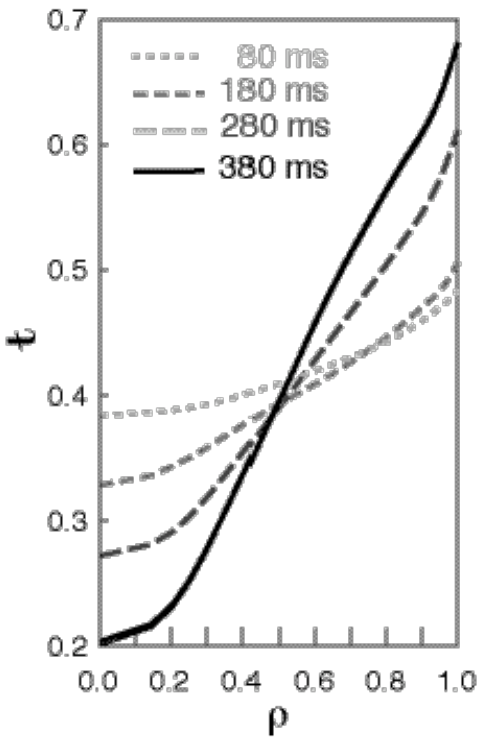

Figure 6. Transform profiles at selected times after optimization on coil currents.